


Morphology of U_3O_8 materials following storage under controlled conditions of temperature and relative humidity

Alison L. Tamasi^{1,2} · Leigh J. Cash¹ · William Tyler Mullen¹ · Alison L. Pugmire¹ · Amy R. Ross¹ · Christy E. Ruggiero¹ · Brian L. Scott¹ · Gregory L. Wagner¹ · Justin R. Walensky² · Marianne P. Wilkerson¹ 

Received: 6 April 2016 / Published online: 5 July 2016
© Akadémiai Kiadó, Budapest, Hungary 2016

Abstract Changes in the visual characteristics of uranium oxide surfaces and morphology following storage under different conditions of temperature and relative humidity may provide insight into the history of an unknown sample. Sub-samples of three α - U_3O_8 materials—one that was phase-pure and two that were phase-impure—were stored under controlled conditions for two years. Scanning electron microscopy was used to image the oxides before and after storage, and a morphology lexicon was used to characterize the images. Temporal changes in morphology were observed in some sub-samples, and changes were greatest following exposure to high relative humidity.

Keywords Chemical speciation · Morphology · Nuclear forensics · Scanning electron microscopy · U_3O_8 · Uranium oxide

Introduction

Temporal changes in the morphology of uranium oxide materials could provide insight into process and/or storage history [1–5]. Process variables inherent in the synthesis of nuclear materials are known to influence the morphology of uranium oxide products [4, 6–15]. In particular, comparison of the morphology of precipitates with those of subsequent calcination products suggests that microstructures of the

precursor precipitates are retained through heat treatment [6–8, 13–16]. A number of studies have shown that U_3O_8 , a common intermediate in the production of nuclear material, generates schoepite phases ($UO_3 \cdot xH_2O$) during storage under higher relative humidities presumably following oxidation and/or hydration [2, 17–19]. It would be valuable to understand the variables contributing to temporally-induced morphology changes, and if any changes occur, the prospect for using the temporal changes in morphology that arise during storage under different conditions for forensic analyses.

The objective of this study is to characterize images of three α - U_3O_8 samples—one phase-pure α - U_3O_8 sample and two phase-impure U_3O_8 samples—prepared from reaction routes used in nuclear conversion processes. These images were collected using scanning electron microscopy (SEM). Sub-samples of the materials were stored under controlled temperature and relative humidity conditions for 2 years. The chemical speciation of these materials and any chemical changes in the materials following storage were detailed previously [2]. The morphology of the materials are characterized using a lexicon of descriptors for assessing any temporal changes [20]. These results are compared with powder X-ray diffraction (p-XRD) patterns and Extended X-ray Absorption Fine Structure (EXAFS) spectra [2].

Experimental

Materials

Uranium U960 Standard Reference Material obtained from the National Bureau of Standards was used in the synthesis of α - U_3O_8 [2]. Ammonium hydroxide (Trace Metal grade),

✉ Marianne P. Wilkerson
mpw@lanl.gov

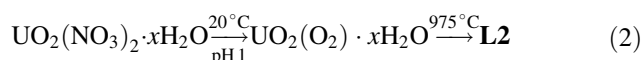
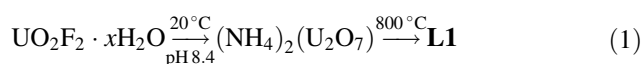
¹ Los Alamos National Laboratory,
P.O. Box 1663, Los Alamos, NM 87545, USA

² Department of Chemistry, University of Missouri-Columbia,
Columbia, MO 65211, USA

concentrated hydrochloric acid (Trace Metal grade), hydrogen peroxide (A.C.S. certified, 30 %), and platinum foil (Alpha Aesar 00261) were purchased from Fisher Scientific and used as received. Lithium iodide and potassium nitrate were purchased from Fisher Scientific and used as received.

Syntheses

The preparation of α - U_3O_8 (**S1**) is described elsewhere [2, 16]. The phase purity was confirmed by p-XRD analysis. This material is a black powder. Legacy materials were retrieved from LANL stock of uranium oxides synthesized on a 10 g scale using reaction routes often used in nuclear fuel processes. Legacy sample 1 (**L1**) and legacy sample 2 (**L2**) were made from these reaction routes:



Both legacy samples are also black powders. The chemical speciation of **L1** and **L2** is detailed elsewhere [2].

Material storage under controlled temperature and relative humidity

Aging vessels fabricated from Swagelok fittings are described elsewhere [1, 2, 21]. The four storage conditions of temperature and relative humidity used in these experiments were: Condition 1 (5 °C and 25 %), Condition 2 (37 °C and 15 %), Condition 3 (5 °C and 97 %), and Condition 4 (37 °C and 89 %). These conditions are listed in Table 1 with respective water vapor densities. A saturated lithium iodide aqueous solution was used to obtain lower relative humidities. A saturated potassium nitrate aqueous solution was used to achieve higher relative humidities. Time 0 for **S1** was the time at which the synthesis of the material was completed. Time 0 for **L1** and **L2** was the time at which each sample was retrieved from storage. Average conditions in our laboratory were 20 °C and ~20 % relative humidity.

Table 1 Conditions (temperature, relative humidity) and resultant water vapor density used for storage of materials [1, 2, 21]

Condition	Temperature (°C)	Relative humidity (%)	Water vapor density (g/cm ³)
1	5	25	1.7×10^{-6}
2	37	15	6.6×10^{-6}
3	5	97	6.7×10^{-6}
4	37	89	39×10^{-6}

Scanning electron microscopy (SEM)

Samples were prepared by dusting the surface of a carbon adhesive disc adhered to an SEM mount with uranium oxide material and then lightly tapping the loose particles away. Images of the samples were collected on an FEI Quanta 200F Field Emission SEM using accelerating voltages of 15–30 kV.

Lexicon

A lexicon was employed to describe the morphology of the materials. The lexicon provides a taxonomic path schematic for the description of particle/subparticle morphology including the surface textures and features observed in an SEM image [20]. Terminology from the lexicon is denoted by italic type face.

Results and discussion

Phase-pure α - U_3O_8

Images of the phase-pure α - U_3O_8 (**S1**) were collected and assessed to benchmark temporal changes in legacy materials **L1** and **L2**. The **S1** was prepared by calcination of $\text{UO}_2(\text{O}_2) \cdot x\text{H}_2\text{O}$ as described in references [2] and [16], and the p-XRD analysis of **S1** revealed that it was phase-pure α - U_3O_8 . An image collected from **S1** is presented in Fig. 1. We found the lexicon useful for describing the morphology of the materials. Freshly-prepared **S1** is characterized as having *clumped/massive agglomerates* composed of sub-particles having a *rounded/sub-rounded* habit of *semi-rounded grains* arranged in *irregular clumps* that are *somewhat rough* and have a similar appearance as the *solution-grown* $\text{UO}_2(\text{O}_2) \cdot x\text{H}_2\text{O}$ (see Table 2) (vide supra). The sub-particles in this image are $>0.5 \mu\text{m}$, but an image of α - U_3O_8 from a replicate synthesis showed the same morphology in sub-particles that were $<0.5 \mu\text{m}$ [16]. Comparison of the images of the precursor $\text{UO}_2(\text{O}_2) \cdot x\text{H}_2\text{O}$ with those of **S1** indicated that morphology was maintained following calcination of the uranyl peroxide precipitate to the uranium oxide product. Further work should be carried out to determine if the particulate size of the precursor is carried over into the calcination product, as well.

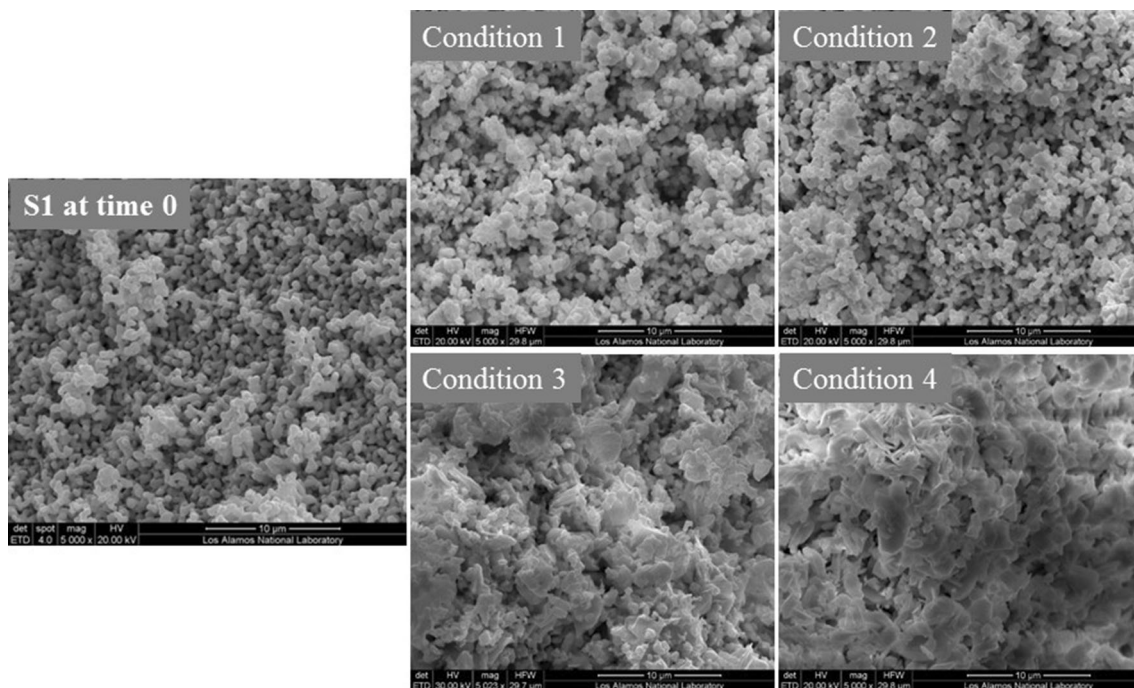


Fig. 1 SEM images of α -U₃O₈ (**S1**) at time 0 [16] (left) and after storage for 2 years under Conditions 1–4 (center and right)

Table 2 Lexicon descriptions and chemical speciation of **S1** at time 0 and after 2 years of storage under Conditions 1–4 [20, 22]

	Time 0	Condition 1	Condition 2	Condition 3	Condition 4
Steps in lexicon	1D. Clumped/massive: agglomerate	1D. Clumped/massive agglomerate	1D. Clumped/massive agglomerate	1D. Clumped/massive conglomerate	1D. Clumped/massive agglomerate
	10. Rounded/sub-rounded	10. Rounded/sub-rounded	10. Rounded/sub-rounded	10. Rounded/sub-rounded	10. Rounded/sub-rounded, platy (some)
	11. Irregular/clumped. Granular: semi-rounded grains	11. Irregular/clumped. Granular: semi-rounded grains	11. Irregular/clumped. Granular: semi-rounded grains	11. Irregular/clumped. Granular: semi-rounded grains	11. Irregular/clumped, scaled (some)
	7. Somewhat rough	7. Somewhat rough	7. Somewhat rough	7. Somewhat rough	7. Somewhat smooth
	8. Other	8. Other	8. Other	8. Surface appearance: eroded	8. Surface appearance: eroded, dissolved
	9. Other: known (calcined from solution-grown precipitate)	9. Other	9. Other	9. Other	9. Other
Chemical speciation [2, 16]	α -U ₃ O ₈	α -U ₃ O ₈	α -U ₃ O ₈	α -U ₃ O ₈ and UO ₃ ·xH ₂ O	α -U ₃ O ₈ and UO ₃ ·xH ₂ O

Notes in the table are provided in parentheses

Sub-samples of **S1** were stored under Conditions 1 through 4 for 2 years after which time images were collected by SEM and characterized using the lexicon (See Table 2) [22]. The SEM images of the aged materials are given in Fig. 1. These images of material stored under lower relative

humidity (Conditions 1 and 2) do not reveal apparent changes in morphology. Little change in chemical speciation of **S1** was measured by p-XRD or EXAFS, either [2]. However, storage of **S1** under higher relative humidity (Conditions 3 and 4) resulted in an apparent flattening of the

habit to an *eroded surface appearance* (Condition 3) or *eroded or dissolved surface appearance* (Condition 4) (See Table 2). Likewise, the p-XRD patterns of **S1** stored under high relative humidity (Conditions 3 and 4) showed the presence of both α - U_3O_8 and schoepite-like species ($\text{UO}_3 \cdot x\text{H}_2\text{O}$), likely due to oxidation and hydration of the initial material [2]. The larger size of the particles in **S1** following storage under Condition 4 is likely due to significant absorption of water. These results are further supported by the EXAFS data which showed that **S1** stored under Condition 4 exhibited the greatest degree of disorder in the local structure compared to material stored under the other conditions (Conditions 1–3.)

Legacy samples

Two legacy samples retrieved from LANL stock were selected for this study because these materials contained chemical impurities that potentially could be incorporated in uranium oxide materials prepared in nuclear processes. For example, the p-XRD pattern of **L1** confirmed the presence of α - U_3O_8 and a measurable amount of $[\text{UO}_2\text{F}_2(\text{H}_2\text{O})](\text{H}_2\text{O})_{0.571}$, which most likely was starting material that prevailed through the precipitation of ammonium diuranate and subsequent calcination to α - U_3O_8 [2]. The p-XRD pattern for **L2** indicated the presence of α - U_3O_8 and a small quantity of schoepite phases, likely due to oxidation and hydration before the sample was retrieved from storage for study.

The SEM images of **L1** and **L2** at time 0 are given in Fig. 2, and the descriptors for **L1** and **L2** are provided in Tables 3 and 4, respectively. The SEM image of **L1** reveals *clumped/massive agglomerates* with a *rounded/sub-rounded* mineral habit of *granular, semi-rounded grains* arranged in *irregular clumps* composed of particles of up to 5 μm diameter, but in comparison with **S1**, the particle

surfaces are *smooth* with *surface decorations* of *finer* that are $<0.5 \mu\text{m}$ diameter. Although these morphologic differences could be dependent upon chemical impurities, it is also possible that they are a result of the morphology of the precursor complex. No images of the precursor complexes were available for comparison, and so conclusive attributions cannot be assigned.

The descriptor for the SEM image of **L2** is different from that for **S1**. The SEM image of **L2** displayed *clumped/massive agglomerates* with *irregular clumps* of particles $<0.5 \mu\text{m}$ diameter.

The images of **L1** post-storage reveal changes in morphology (See Fig. 3) and chemical speciation. Following storage for 2 years under the low relative humidity Condition 1, the morphology took on *clumped/massive* sub-particles in a *bimodal* distribution of *rounded/sub-rounded* habit of *granular, semi-rounded grains* of *irregular* and *smooth* particles. The material stored under Condition 2 appears to be a *conglomerate* of *sub-rounded clumps* with a *somewhat rough surface*. A sample of **L1** was not stored under Condition 3. The most visible change was in the images of material stored under Condition 4, which is best described by a different description path through the lexicon [20]. The morphology appears to be a *complex conglomerate* that was a *mixture* of *sub-angular/angular* and other particles. One portion of the particles looks to have *high sphericity flattened* and *blocky irregular plates*, with a *smooth surface*, while the other portion consists of *subhedral* and *bladed plates* with a *smooth surface*. The initial uranyl fluoride impurity was not measurable by p-XRD analysis after 2 years, perhaps through decomposition to another chemical species or due to masking by more predominant lines.

Images of the **L2** material after storage for 2 years under Conditions 1–4 are given in Fig. 4. Powder-XRD analysis of these materials all show the presence of α - U_3O_8 and

Fig. 2 SEM images of **L1** (α - U_3O_8 and $[\text{UO}_2\text{F}_2(\text{H}_2\text{O})](\text{H}_2\text{O})_{0.571}$) (left) and **L2** (α - U_3O_8 and $\text{UO}_3 \cdot x\text{H}_2\text{O}$) (right) at time 0

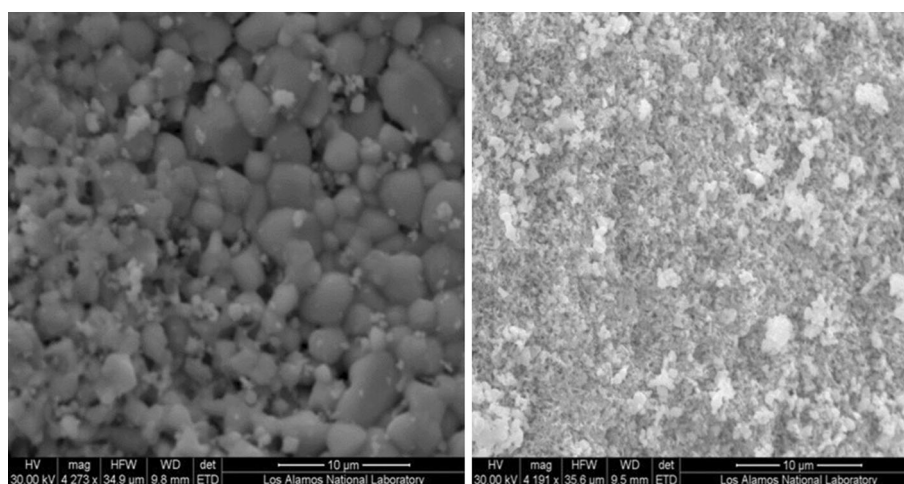


Table 3 Lexicon descriptions and chemical speciation of **L1** (α -U₃O₈ and [UO₂F₂(H₂O)](H₂O)_{0.571}) at time 0 and after 2 years of storage under Conditions 1, 2 and 4

	Time 0	Condition 1	Condition 2	Condition 4	
Steps in lexicon	1D. Clumped/massive: agglomerate	1D. Clumped/massive: bimodal	1D. Clumped/massive: conglomerate	1B. Complex particles: conglomerate	
	10. Rounded/sub-rounded	10. Rounded/sub-rounded	10. Sub-rounded	2. Mixture	
	11. Irregular/clumped. Granular: semi-rounded grains	11. Irregular/clumped. Granular: semi-rounded grains	11. Clumped	3. Sub-angular/ angular	N/A
	N/A	N/A	N/A	4. High sphericity: flattened/blocky	N/A
	N/A	N/A	N/A	N/A	5. Subhedral
	N/A	N/A	N/A	N/A	6. Platy/plate/ bladed
	7. Smooth	7. Smooth	7. Somewhat rough	7. Smooth	7. Smooth
	8. Surface decorations: fines	8. Other	8. Other	8. Other	8. Other
	9. Other: known (calcined)	9. Other	9. Other	9. Other	9. Other
	N/A	N/A	N/A	10. Platy	10. Platy
	N/A	N/A	N/A	11. Irregular	11. Irregular
Chemical speciation [2, 16]	α -U ₃ O ₈ (major) and [UO ₂ F ₂ (H ₂ O)](H ₂ O) _{0.571} (minor)	α -U ₃ O ₈ and UO ₃ ·xH ₂ O	α -U ₃ O ₈ and UO ₃ ·xH ₂ O	α -U ₃ O ₈ and UO ₃ ·xH ₂ O	

Notes in the table are provided in parentheses

N/A not applicable

Table 4 Lexicon descriptions and chemical speciation of **L2** (α -U₃O₈ and UO₃·xH₂O) at time 0 and after 2 years of storage under Conditions 1–4

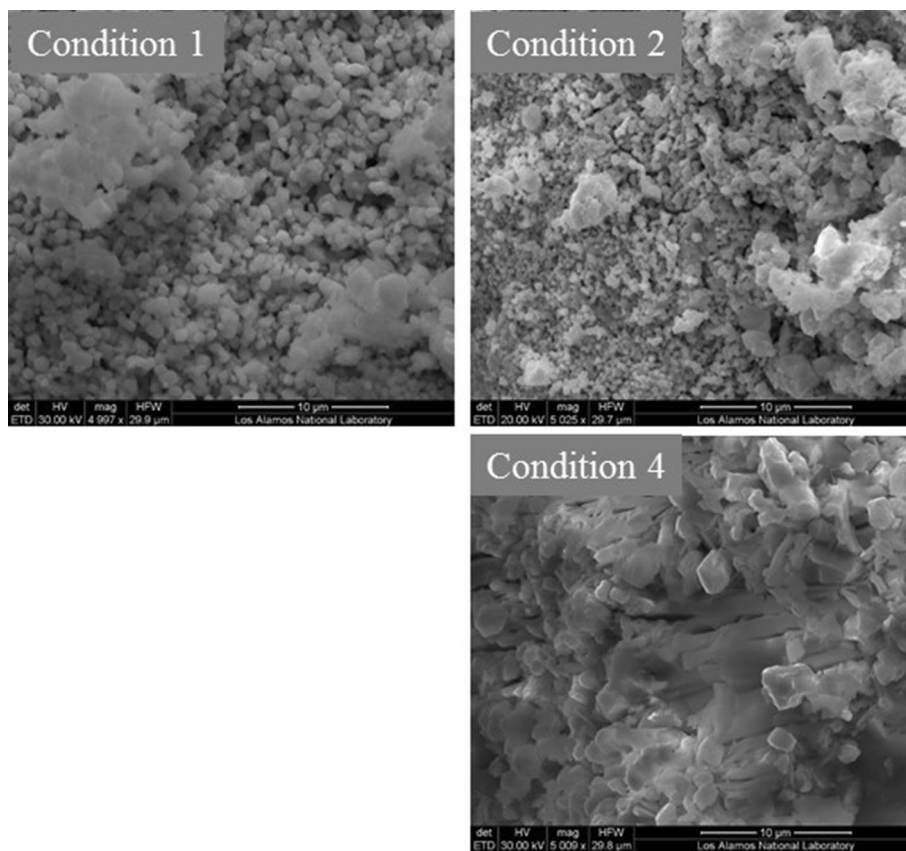
	Time 0	Condition 1	Condition 2	Condition 3	Condition 4
Steps in lexicon	1D. Clumped/massive: agglomerate	1D. Clumped/massive: conglomerate	1D. Clumped/massive: agglomerate	1D. Clumped/massive: conglomerate	1D. Massive: conglomerate
	10. Other	10. Sub-rounded	10. Other	10. Sub-rounded	10. Other
	11. Irregular/clumped	11. Irregular/clumped	11. Irregular/clumped	11. Irregular/clumped	11. Irregular/clumped
	7. (indeterminate)	7. Smooth	7. Somewhat rough	7. Smooth	7. Rough
	8. Other	8. Surface decorations: fines, scale	8. Other	8. Surface appearance: dissolved	8. Surface indentations: pored
	9. Other: known (calcined)	9. Other	9. Other	9. Other	9. Other
Chemical speciation [2, 16]	α -U ₃ O ₈ (major) and UO ₃ ·xH ₂ O (minor)	α -U ₃ O ₈ and UO ₃ ·xH ₂ O	α -U ₃ O ₈ and UO ₃ ·xH ₂ O	α -U ₃ O ₈ and UO ₃ ·xH ₂ O	α -U ₃ O ₈ and UO ₃ ·xH ₂ O

Notes in the table are provided in parentheses

UO₃·xH₂O phases, likely inter-grown metaschoepite and schoepite patterns that cannot be resolved [19]. It is not possible to determine if either the schoepite phases are redistributing between different schoepite phases without changing the ratio of UO₃:H₂O due to dissolution and

precipitation during storage over this time, or progressing from one schoepite phase to another. Material stored under the lower temperature conditions (1 or 3) appears to be *clumped/massive conglomerates* of *sub-rounded* and *irregular clumps* that included *fines and scale decorations*

Fig. 3 SEM images of **L1** (α - U_3O_8 and $[\text{UO}_2\text{F}_2(\text{H}_2\text{O})](\text{H}_2\text{O})_{0.571}$) after storage for 2 years under Conditions 1, 2, and 4



(Condition 1) or a *dissolved surface appearance* (Condition 3). The material stored under Condition 2 is a *massive agglomerate of irregular clumps with a somewhat rough surface*. In contrast, the image of material stored under Condition 4 exhibits a *massive conglomerate of irregular clumps with a somewhat rough surface containing pored surface indentations*. The formation of this texture could have formed from rapid absorption followed by desorption of water [1, 2].

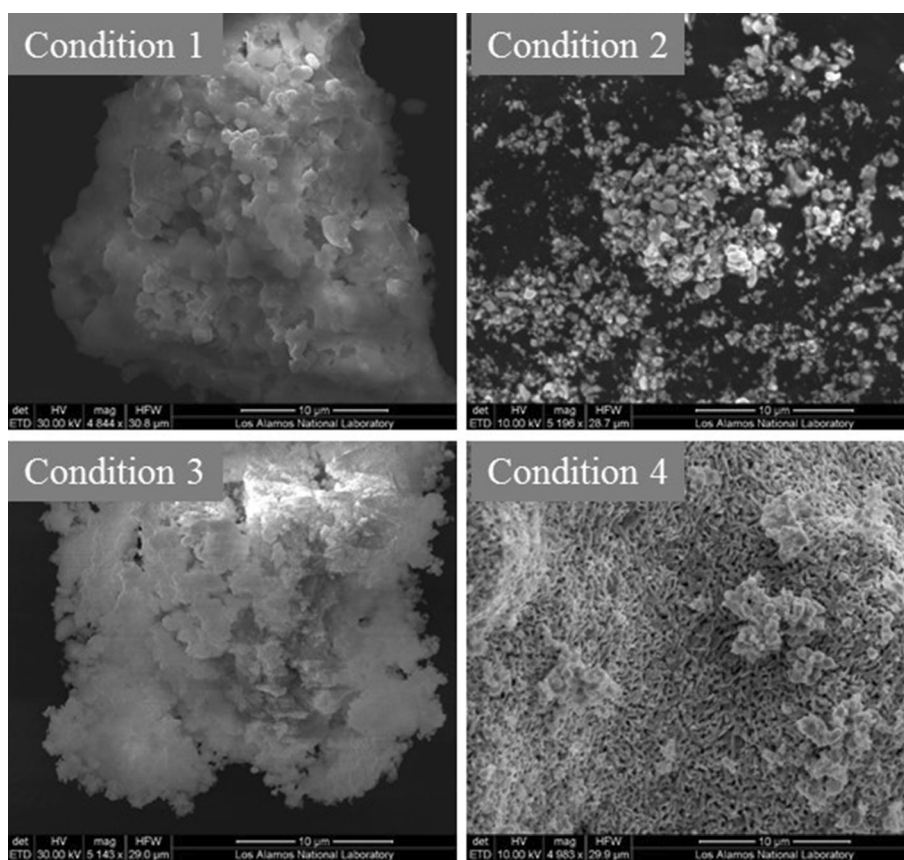
Image of **S1**, **L1**, and **L2** reveal that changes in the morphology were particularly notable following storage under higher relative humidity and temperature (Condition 4). Although the same conditions were employed for storage of **S1**, **L1**, and **L2** over 2 years, however, the changes in morphology of materials with impurities (**L1** and **L2**) were more obvious than the changes in the morphology of phase-pure **S1**. It is possible that chemical impurities present in **L1** and **L2** at time 0 were responsible for the more significant changes in morphology. Research into uranium oxide materials has suggested that relatively minor shifts in localized environment affect the growth of crystals [23]. It also has been shown that doping more oxidized uranium oxides, such as U_3O_8 , into UO_2 powder influences grain size and packing during sintering [24, 25]. While not actinide systems, other studies of transition species in the Cd-I-Cu system have demonstrated that the

impurities in copper compounds promote preferential growth directionality along surface planes, consistent with our results here, while other work has revealed the effect of chemical impurities on nucleation and growth of ettringite in a concrete environment. [26, 27]. Alternatively, materials **L1** and **L2** had already begun oxidation and hydration before they were removed from storage, which may have induced a more rapid change over this 2 year time period under high relative humidity.

Conclusions

An understanding of the potential for changes in morphology in uranium oxide materials over time and correlation of temporal changes in morphology with chemical speciation would be valuable for understanding the history of unknown analogues and/or evaluating morphology. Previous work to characterize U_3O_8 has shown that chemical signatures incorporated from a nuclear fuel process or produced following storage under controlled temperature and relative humidity over time may be measurable by p-XRD analysis. Additional characterization using p-XRD analysis and EXAFS spectroscopy has given a better understanding of the extent of oxidation and hydration in U_3O_8 following storage. Here, we collected

Fig. 4 SEM images of L2 (α - U_3O_8 and $\text{UO}_3 \cdot x\text{H}_2\text{O}$) after storage for 2 years under Conditions 1–4



images from the phase-pure material and two of the phase-impure materials from the previous study. The three materials were stored under different conditions of temperature and relative humidity over 2 years. The images of the phase-pure material showed little or no changes in morphology following storage under low relative humidity. While images of all materials revealed greater changes in morphology following storage under the higher relative humidity conditions, phase-impure materials yielded more discernable changes in mineral habit after storage for 2 years. These results suggest changes in surface area of the materials, which could provide another forensic signature of material storage history. Although these results do not elucidate these processes, these results suggest the need to conduct further studies to evaluate potential changes in morphology and particle sizes along with chemical speciation using uranium oxide materials with known quantities of impurities.

Acknowledgments This work has been supported by the U.S. Department of Homeland Security, Domestic Nuclear Detection Office, Transformational and Applied Research Directorate and National Technical Nuclear Forensics Center, under competitively awarded contracts IAA HSHQDC-13-X-00269 and under HDHQDC-08-X-00805. ALT gratefully acknowledges the U.S. Department of Homeland Security under Grant Award Number, 2012-DN-130-NF001-02, the Seaborg Institute, and the University of Missouri for

providing funding to perform this work. J.R.W.'s contribution to this material is based upon work supported by the U.S. Department of Homeland Security under Grant Award Number, 2012-DN-130-NF001-02. The views and conclusions contained in this document are those of the authors and should not be interpreted as necessarily representing the official policies, either expressed or implied, of the U.S. Department of Homeland Security or the Government. Los Alamos National Laboratory is operated by Los Alamos National Security, LLC, for the National Nuclear Security Administration of U.S. Department of Energy (contract DE-AC52-06NA25396). The authors declare no competing financial interests. LA-UR-16-21674.

References

1. Wagner G, Kinkead S, Paffett M, Rector K, Scott B, Tamasi A, Wilkerson M (2015) Morphologic and chemical characterization of products from hydrolysis of UF_6 . *J Fluorine Chem* 178:107–114
2. Tamasi A, Boland K, Czerwinski K, Ellis J, Kozimor S, Martin R, Pugmire A, Reilly D, Scott B, Sutton A, Wagner G, Walensky J, Wilkerson M (2015) Oxidation and hydration of U_3O_8 materials following controlled exposure to temperature and humidity. *Anal Chem* 87:4210–4217
3. Mayer K (2013) Expand nuclear forensics. *Nature* 503:461–462
4. Mayer K, Wallenius M, Varga Z (2013) Nuclear forensic science: correlating measurable material parameters to the history of nuclear material. *Chem Rev* 113:884–900
5. Joint Working Group of the American Physical Society and the American Association for the Advancement of Science: Nuclear

- Forensics: Role, State of the Art, Program Needs. http://www.aaas.org/sites/default/files/migrate/uploads/Nuclear_Forensics.pdf
- Paik S, Biswas S, Bhattacharya S, Roy S (2013) Effect of ammonium nitrate on precipitation of ammonium di-uranate (ADU) and its characteristics. *J Nucl Mater* 440:34–38
 - Manna S, Roy S, Joshi J (2012) Study of crystallization and morphology of ammonium diuranate and uranium oxide. *J Nucl Mater* 424:94–100
 - Manna S, Karthik P, Mukherjee A, Banerjee J, Roy S, Joshi J (2012) Study of calcinations of ammonium diuranate at different temperatures. *J Nucl Mater* 426:229–232
 - Andreev E, Glavin K, Ivanov A, Malovik V, Martynov V, Panov V (2009) Some results uranium dioxide powder structure investigation. *Russ J Non Ferrous Met* 50:281–285
 - Marajofsky A, Perez L, Celora J (1991) On the dependence of characteristics of powders on the AUC process parameters. *J Nucl Mater* 178:143–151
 - Pan Y-M, Ma C-B, Hsu N-N (1981) The conversion of UO_2 via ammonium uranyl carbonate: study of precipitation, chemical variation and powder properties. *J Nucl Mater* 99:135–147
 - Woolfrey J (1978) The preparation of UO_2 powder: effect of ammonium uranate properties. *J Nucl Mater* 74:123–131
 - Janov J, Alfredson P, Vilkaitis V (1972) The influence of precipitation conditions on the properties of ammonium diuranate and uranium dioxide powders. *J Nucl Mater* 44:161–174
 - Cordfunke E, van der Giessen A (1967) Particle properties and sintering behaviour of uranium dioxide. *J Nucl Mater* 24:141–149
 - Doi H, Ito T (1964) Significance of physical state of starting precipitate in growth of uranium dioxide particles. *J Nucl Mater* 11:94–106
 - Tamasi A, Cash L, Mullen W, Ross A, Ruggiero C, Scott B, Wagner G, Walensky J, Zerkle S, Wilkerson M (2015) Comparison of morphologies of a uranyl peroxide precursor and calcination products. *J Radioanal Nucl Chem* doi:10.1007/s10967-016-4692-x
 - He H, Wang P, Allred D, Majewski J, Wilkerson M, Rector K (2012) Characterization of chemical speciation in ultrathin uranium oxide layered films. *Anal Chem* 84:10380–10387
 - Lloyd N, Mosselmans J, Parrish R, Chenery S, Hainsworth S, Kemp S (2009) The morphologies and compositions of depleted uranium particles from an environmental case-study. *Mineral Mag* 73:495–510
 - Finch R, Hawthorne F, Ewing R (1998) Structural relations among schoepite, metaschoepite and “dehydrated schoepite”. *Can Mineral* 36:831–845
 - Tamasi A, Cash L, Eley C, Porter R, Pugmire D, Ross A, Ruggiero C, Tandon L, Wagner G, Walensky J, Wall A, Wilkerson M (2016) A lexicon for consistent description of material images for nuclear forensics. *J Radioanal Nucl Chem* 307:1611–1619
 - Anovitz L, Riciputi L, Cole D, Gruszkiewicz M, Elam J (2006) The effect of changes in relative humidity on the hydration rate of Pachuca obsidian. *J Non-Cryst Solids* 352:5652–5662
 - Wilkerson M, Kinman W, Kozimor S, Pugmire A, Scott B, Tamasi A, Wagner G, Walensky J (2014) Probing forensic signatures of nuclear materials. In: Proceedings in the IAEA international conference on advances in nuclear forensics (IAEA-CN-218) Vienna, Austria, 7–10 July 2014
 - Pradhan M, Sarkar S, Sinha A, Basu M, Pal T (2011) Morphology controlled uranium oxide hydroxide hydrate for catalysis, luminescence and SERS studies. *Cryst Eng Comm* 13:2878–2889
 - Petrov I, Basov V (2009) Investigation of the influence of the initial state of powder, pore-forming additions, and U_3O_8 on the microstructure and strength of fuel pellets. *At Energ* 107:85–88
 - Kang K, Yang J, Kim J, Rhee Y, Kim D, Kim K, Song K (2008) Improvement of UO_2 pellet properties by controlling the powder morphology of recycled U_3O_8 powder. *J Nucl Sci Technol* 45:1150–1154
 - Ithnin R, Jones R (1996) CdI_2 single-crystal growth on $\text{Cu}(111)$: adsorption, desorption and formation of a chemisorbed CdI_1 phase. *J Phys: Condens Matter* 8:3285–3295
 - Cody A, Lee H, Cody R, Spry P (2004) The effects of chemical environment on the nucleation, growth, and stability of ettringite $[\text{Ca}_3\text{Al}(\text{OH})_6]_2(\text{SO}_4)_3 \cdot 26\text{H}_2\text{O}$. *Cem Concr Res* 34:869–881